V2G Ancillary Services Management Strategy for EVs with Solar Powered Charging Stations Based on Artificial Intelligence Algorithms

Semaria Ruiz-Alvarez*‡ ⓘD , Jesus Hernandez ** ⓘD , David Borge-Diez *** ⓘD

*Department of Energy and Processes, Universidad Nacional de Colombia, Medellín, zip code: 050034, Antioquia, Colombia.

**Electric Energy and Automation Department of Universidad Nacional de Colombia, Medellín, zip code: 050034, Antioquia, Colombia.

*** Electrical, Systems and Automation Engineering Department, University of León, León, zip code: 24007., León, España.

(seruizal@unal.edu.co, jahernan@unal.edu.co, david.borge@unileon.es)

‡ Corresponding Author, Medellin, Colombia.

seruizal@unal.edu.co

Abstract- This research proposes a vehicle-to-grid strategy based on dynamic optimization for a fleet of public transportation Electric Vehicles (EVs) whose charging station is jointly powered by the conventional electrical network and photovoltaic renewable sources. Utilizing two neural networks, the proposed algorithm predicted future energy expenditure of Electric Vehicles (EVs) and the power generation potential of the renewable sources. The goal was to optimize dynamically the EVs' decision-making, encompassing their charging-discharging schedules, power exchange with the electrical network, and travel dispatch. The analysis considered the EVs' capacity for selling energy and providing frequency reserve ancillary services. Consequently, this proposal enables the estimation of fleet management plans by considering the daily average congestion level in the analysis zone, the required departure schedules of the vehicles in the fleet, and the past measures of solar radiation at the site. These variables serve as inputs for the prediction algorithms. The mathematical model of dynamic optimization was formulated as a convex Mixed-Integer problem and was solved using the iterative branch and cut method. The findings revealed that the most profitable options for the EVs' owners include selling energy and providing downward regulation ancillary services. Moreover, as the solution's viability relied on the accuracy of the prediction algorithms' outputs, two high precision neural networks, with an error rate lower than 2%, have been employed.

Keywords: Artificial Intelligence, Electric Vehicles, Neural Networks, Optimization methods, Renewable Energy Sources, Vehicle-to-Grid.

1. Introduction

Currently, the research on electric vehicles contributing storage-based ancillary services to the electrical network has gained significant relevance. EV batteries, utilized during parking periods, offer opportunities to provide frequency regulation, voltage support, or to smooth intermittencies of renewable sources, among other services [1]. As power systems with a high penetration of distributed highly variant sources and EVs suffer of huge effects in the electricity network operation [2], [3]. Hence, it is indispensable to have management strategies that coordinate the transport services with ancillary services supplying [4]–[6]. In this regard, the current research proposes an optimization and artificial intelligence-based management strategy applicable to public transport EVs fleets. It is motivated in the fact that the replacement of conventional (fuel based) vehicles for public transport by EVs, is a practice that has been increasing around the world, as it can avoid the production of CO_2 derived from the fossil fuels usage.

Furthermore, the proposed strategy extend the approaches presented in the previous researches [7], [8] which are based

on the EVs batteries aggregation approach, and the works presented in [5], [9]–[13], by providing charging/discharging plans for individual EVs and also allocating specific travel assignments to each vehicle within the fleet. This comprehensive approach considers the EVs' capability to offer secondary frequency regulation reserves and engage in energy sales to the electrical network, while incorporating renewable energy sources at the charging stations. In addition, it provides the management plans for individual EVs instead of for the whole aggregated fleet as in the references [7], [8]. Having also as a novelty, the addition of two estimation modules that provide the decision-making system inputs, which are intended to forecast the energy expenditure in travels and the renewable power generation, instead of using fixed energy expenditure profiles as in [14]. Particularly, the energy expenditure estimation module uses a backpropagation neural network whose architecture was inspired in the work [15], which takes as inputs the average daily congestion level in the traffic region and the starting hour of the required travels. This estimation algorithm eliminates the need for energy meters onboarding of EVs and relates energy consumption to variables commonly available for operators of public transport fleets. And, specifically, it poses an advantage regarding the method set in work [15], since it allows the fleet operator to make its decisions based on the congestion expected for a specific day. Being the congestion a critical issue for the study case traffic network, located at Medellín Colombia, as it is indicated in [16].

Furthermore, the renewable generation forecasting module uses a Long short-term memory neural network, which is able to capture dependencies in time of the input variables and is used to predict highly variant time series [17], [18].

Therefore, in the proposed strategy both prediction modules are set together with the decision-maker that takes as inputs the forecasted variables and executes a convex Mixed-Integer Dynamic (MID) optimization to find the most economically profitable decisions for each EV in the fleet; where the cost function of the decision-maker is composed by the daily cash flow for the EVs owners, generated by the energy purchases, sales, ancillary services provision payments, and the batteries wear cost. The mathematical approach of this procedure is described in Section 2. Sections 3 and 4 detail the algorithms of the estimation modules. Finally, Section 5 describes the study case and the results found with the solution of the optimization problem, which is carried out using the iterative method branch and cut.

2. EVs Management Proposal

The EVs management strategy proposed was applied to control the charging/discharging processes of the EVs fleet and schedule their travels. It is based on dynamic Mixed-Integer convex optimization executed online for each time step k, with a daily horizon. The traffic system under consideration is a public EVs system, with a single charging station and composed of electric buses. In this system, the vehicles parked at the charging station can sell energy and provide upward and downward frequency regulation services to the electrical power network.

More precisely, the upward regulation, denoted as $P_{d,ru}$ was associated with the cases in which the Transmission System Operator - TSO (in charge of managing the activation of the frequency regulation ancillary services) requires that EVs deliver more discharging power than those they have scheduled for selling to the electrical network.

Similarly, the downward regulation, denoted as $P_{c,rd}$, was linked to the situations in which the TSO requires that the EVs decrease their charging power. Moreover, the proposed dynamic optimization strategy takes as input data the estimated initial state of charge of EVs, the estimated energy expenditure during travels, and the estimated energy generated by renewable sources located at the charging stations. We detail the procedure to obtain the last two estimated inputs in section 3 and 4, which relies on AI algorithms. Furthermore, the proposed strategy gives as output, the charging/discharging plans for each EV in the fleet, and the assignment of each required travel to a specific EV in the fleet, maximizing the EVs aggregator incomes and minimizing its operative costs.

A schematic view of the proposed strategy is show in Fig. 1 and hence, the dynamic model for the energy content of the EVs batteries, indicated in Eq. (1), is used to obtain the optimization policy that will govern the block "charging/discharging and travel scheduling strategy".

$$E^j(k+1) = (1 - \sigma_b)E^j(k) + P_c^j(k) - P_d^j(k) \qquad (1)$$

And, considering a maximum capacity E^M for the EVs batteries, the state of charge of the batteries can be estimated with the expression of Eq. (2).

$$SOC^j(k) = \frac{E^j(k)}{E^M} \qquad (2)$$
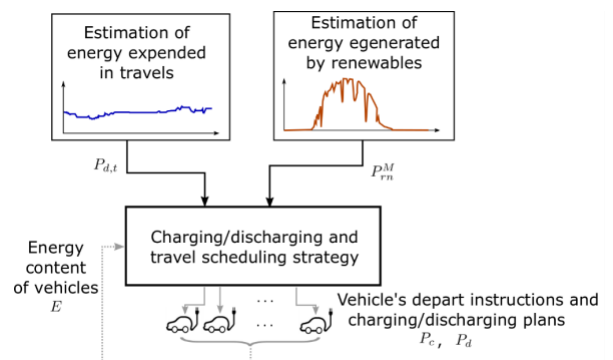
Figure 1. Scheme of the proposed fleet management strategy for the aggregator.

where the element $P_d^j(k)$ corresponds to the discharging power of the j-th battery at the k-th time step.

The variable P_d is divided into three new variables: $P_{d,g}, P_{d,t}, P_{d,ru}$ as the discharging power can be due to the vehicle traveling $P_{d,t}$, to a power exchanging with the electric network $P_{d,g}$, or to the provision of the upward regulation service $P_{d,ru}$. Hence the variable P_d will be calculated as indicates Eq. (3).

$$P_d = P_{d,g} + P_{d,t} + P_{d,ru} \qquad (3)$$

In a similar way, the variable P_c is obtained as the sum of the three new variables $P_{c,g}$, $P_{c,rd}$, $P_{c,rn}$ which represent the power purchased from the electrical network, the downward regulation service scheduled, and the power generated by the renewable sources, respectively. Therefore, the variable P_c is obtained with (4).

$$P_c = P_{c,g} + P_{c,rd} + P_{c,rn} \qquad (4)$$

On the other hand, the cost function $f(\cdot)$ for the proposed optimization strategy is set in Eq. (5). It corresponds to the daily cash flow for the EVs aggregator, which includes the purchase energy costs, the revenues from energy sales, the revenues from downward and upward regulation ancillary services provision, and the batteries wear cost.

$$f(P_{c,g}, P_{c,rd}, P_{d,g}, P_{d,ru}, SOC) = C_c \sum_{j=1}^{v} P_c^j - R_d \sum_{j=1}^{v} P_d^j$$
$$-R_{rd} \sum_{j=1}^{v} P_{c,rd}^j - R_{ru} \sum_{j=1}^{v} P_{d,ru}^j + \sum_{j=1}^{v} w(SOC^j) \qquad (5)$$

where v is the amount of EVs in the fleet, and $w(\cdot)$ is the batteries wear function, which is convex. A detailed description of this function is given in reference [7].

Note that the renewable generation is not included in the cost function of Eq. (5), since it is considered, the renewable sources are already installed at the charging station. Hence, their installation costs are omitted, and their operative costs are assumed to be zero. Thus, the system will be intended to use as much renewable energy as possible, because these sources will be free of charge.

Outlining, the complete dynamic optimization approach used in the block "charging/discharging and travel scheduling strategy" of Fig. 1, is described by Eq. (6) and subsequent Eqs. (6a) – (6k).

$$\min_{P_{c,g}, P_{c,rd}, P_{d,rn}, P_{d,g}, P_{d,ru}, P_{d,t}, A_v, A_c} f(P_{c,g}, P_{c,rd},$$
$$P_{d,g}, P_{d,ru}, SOC) \qquad (6a)$$

Subject to

$$1 \cdot SOC^m \leq SOC^j \leq 1,$$
$$1 \cdot E^M \cdot SOC^m \leq E_{rd}^j \leq 1 \cdot E^M,$$
$$1 \cdot E^M \cdot SOC^m \leq E_{ru}^j \leq 1 \cdot E^M, \qquad (6b)$$
$$1 \cdot E^M \cdot SOC^m \leq E_{ru,rd}^j \leq 1 \cdot E^M,$$

$$\sum_{j=1}^{v}(P_{c,g}^j + P_{c,rd}^j) \leq 1 \cdot P_l^M, \qquad (6c)$$

$$\sum_{j=1}^{v}(P_{d,g}^j + P_{d,ru}^j) \leq 1 \cdot P_l^M, \qquad (6d)$$

$$P_{c,g}^j + P_{c,rd}^j + P_{c,rn}^j \leq P^M \cdot A_c^j, \qquad (6e)$$

$$P_{d,g}^j + P_{d,ru}^j \leq 1 \cdot P^M \cdot (1 - A_c^j - u^j), \quad \forall j \in V \qquad (6f)$$

$$\sum_{i=1}^{r} A_{v(i)} = 1 \qquad (6g)$$

where $V = \{1, \cdots, v\}$ is a set containing the indexes of each EV in the fleet, and $N = \{1, \cdots, n\}$ is a set containing the indexes of the time discretization slots in the prediction horizon.

The decision variables of the dynamic optimization problem of Eq. (6) are the matrices $P_{c,g} \in \mathbb{R}^{n \times v}$ which depicts the charging amount of each EV in the fleet at each time step, $P_{c,rd} \in \mathbb{R}^{n \times v}$ which contains the amount of downward reserve provided by each EV at each time step, $P_{c,rn} \in \mathbb{R}^{n \times v}$ that indicates the amount of renewable generation stored in each EV's battery at each time step, $P_{d,g} \in \mathbb{R}^{n \times v}$ that contains the power sold to the electrical network by each EV in the fleet at each time step, $P_{d,ru} \in \mathbb{R}^{n \times v}$ which contains the amount of upward reserve provided by each EV at each time step, $P_{d,t} \in \mathbb{R}^{n \times v}$ which contains the energy expended by each EV performing a travel at each time step, $A_c \in \mathbb{R}^{n \times v}$ which is a binary matrix that indicates the charging periods for each EV (contains 1's at time steps in which batteries are charging and 0 otherwise), and $A_v \in \mathbb{R}^{r \times v}$ which is a binary matrix that indicates the travels performed by each EV: an element (i,j) with value of 1 indicates that the i-th travel is performed by the j-th EV. The elements of those matrices are constrained to be positive.

Moreover, the constraints (Eq. (6b)) are related with the energy limits in the EVs batteries, being SOC^m their minimum allowed state of charge; and considering that the state of charge should lie inside the allowed limits with and without the provision of reserve the ancillary services. Since, independently whether the frequency reserves are effectively used or not, the EVs should have the capacity to supply the energy for required travels. Therefore, the constraints over new variables E_{rd}, E_{ru}, and $E_{ru,rd}$ calculated with Eq. (7) and subsequent Eqs. (7a) – (7c), are included to guarantee these requirements.

$$E_{rd}^j(k+1) = E_{rd}^j(k)(1-\sigma_b) + P_{c,g}^j(k) + P_{c,rn}^j(k) - P_{d,g}^j(k) - P_{d,t}^j(k) -$$
$$P_{d,ru}^j(k) \qquad (7a)$$

$$E_{ru}^j(k+1) = E_{ru}^j(k)(1-\sigma_b) + P_{c,g}^j(k) + P_{c,rn}^j(k) + P_{c,rd}^j(k) - P_{d,g}^j(k) - P_{d,t}^j(k) \qquad (7b)$$

$$E_{ru,rd}^j(k+1) = E_{ru,rd}^j(k)(1-\sigma_b) + P_{c,g}^j(k) + P_{c,rn}^j(k) - P_{d,g}^j(k) - P_{d,t}^j(k) \qquad (7c)$$

Being E_{rd} the energy content in the batteries without considering the downward reserve, E_{ru} the energy content in the batteries without considering the upward reserve, and $E_{ru,rd}$ the energy content in the batteries without considering the downward and upward reserves.

The constraint (Eq. (6c)) represents the limit over the total charging power of the EVs; which must be lower or equal to the rated power capacity of the distribution system lines P_l^M. And in the same way, the constraint (Eq. (6d)) represents the limit over the total discharging power of the EVs.

The constraints of Eqs. (6e) – (6f) are intended to limit the amount of charging/discharging power of each EV according to the rated power capacity of the batteries P^M. Furthermore, we have multiplied this rated capacity by the matrix A_c in the Eq. (6e), which constraints the vehicles to be charged only at time steps in which the binary matrix A_c contains 1's. Similarly, in Eq. (6.f) the discharging process of the vehicles is limited to the time intervals in which they are not being charged or driven to perform travels; such condition was implemented through the multiplication of the term P^M by $(\mathbf{1} - A_c^j(k) - u^j(k))$; where the binary matrix $u \in \mathbb{R}^{n \times v}$ (that contains 1's at the time steps in which EVs performs a travel) is calculated with the Eq. (8).

$$u = (A_v \cdot A_t^T)^T \tag{8}$$

The matrices u and A_c are mutually excluding according to the constraint of Eq. (6i), that implies that vehicles cannot be charged while they are performing a travel.

On the other hand, the constraints of Eqs. (6g) – (6h) are intended to assign the energy consumption of a travel for the vehicle selected to perform it. Particularly, this selection is carried out as Eq. (9) indicates, multiplying the matrix that contains all the estimated power consumption of travels at each time step F_t by the selection matrix A_v, that assigns the power consumption of a travel to a specific EV in the fleet. Considering also that each travel needs to be performed by only one vehicle in the fleet. Such condition is reflected in Eq. (6g).

$$P_{d,t} = F_t \cdot A_v \tag{9}$$

Finally, the constraint of Eq. (6j) established that the total renewable power used to charge the battery of each vehicle need to be equal to the renewable power generation P_{rn}^M.

3. Characterization of EVs Consumption Profiles

As mentioned in the preceding section, the variable corresponding to the energy consumption profiles for each travel required is $F_t \in \mathbb{R}^{n \times r}$, which is an input of the optimization set in Eq. (6). This variable represents the integral of the power consumption in a travel during the time period *[k-1,k]*.

Consider the power consumption denoted as P_{it} which is sampled with a frequency of z; therefore, the energy is obtained as the integral of the power between *[k-1,k]* with Eq. (10).

$$F_t(k,x) = \sum_{z=k}^{k+1} P_{it}(z,x), \text{ for } z \leq k, \text{ for } x \in R \tag{10}$$

Hence, it is necessary to estimate the power consumption of EVs in the defined route, to compute. Here, this task was carried out using an Artificial Intelligence (IA) algorithm that predicts the power consumption of EVs for different departing times of the EVs and different daily average congestion regimes. This AI algorithm was trained with the data obtained from a traffic microsimulation of the study case public transport system under different traffic congestion conditions. The proposed neural network adopts a Backpropagation Network (BPN) architecture featuring one hidden layer housing 17 neurons, which is illustrated in Fig. 2. This architecture has been inspired by the approach proposed in reference [15], and the number of neurons in the hidden layer was determined in such a way the obtained Minimum Square Error (MSE) given by Eq. (11) was the minimum possible.

$$MSE = \frac{1}{N_s} \sum_{j=1}^{4} \sum_{k=1}^{N_s} \left(Y_j(k) - \widehat{Y}_j(k) \right)^2 \tag{11}$$

Where $\widehat{Y}_j(k)$ is the estimated value of the output variables calculated with the Neural Network.
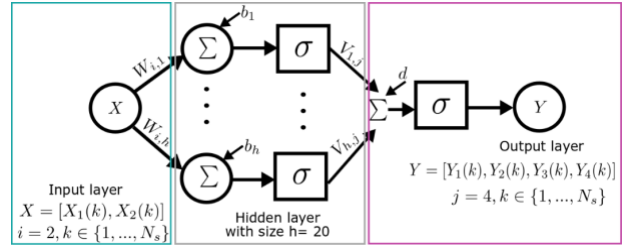
Figure 2. Backpropagation neural network architecture for the EVs energy consumption prediction.

Where the input layer has a data set X with 2 features: the starting hour of the travel and the congestion level; and $N_s = 4914$ samples. And the output layer gives a dataset $Y \in \mathbb{R}^{4 \times 4914}$, for which, the 4 features correspond to the energy consumption at each time step, considering steps length of 5 minutes and a maximum travel duration of 20 minutes.

Moreover, the values b_i, W_{ij}, V_{ij}, d, and σ are the input bias factors, the input weight matrix, the output weight matrix, the output bias factor, and the sigmoidal activation function, respectively.

Fig. 3 depicts the obtained results for the prediction of EVs energy consumption applying the backpropagation NN to the transport system of the study case, considering different traffic congestion cases (of 80% for high congestion, and 20% for low congestion). Here it can be observed that the high congestion case implies high energy consumption at the peak hours (6:00-7:00 h, 16:00, and 18:00).
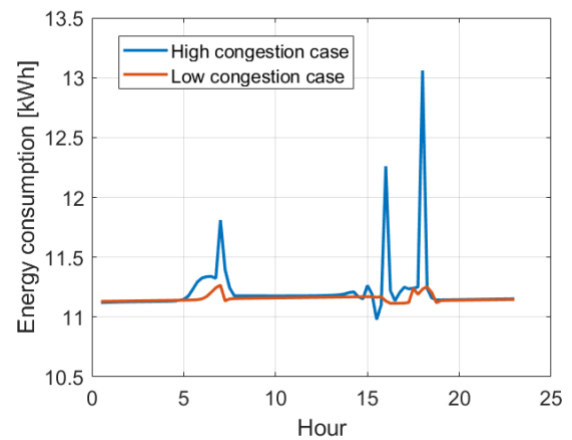
Figure 3. Predicted energy consumption of the EVs obtained with the backpropagation neural network.

On the other hand, the obtained prediction accuracy, i.e., the MSE error of the training set was 0.12%; which is consider

acceptable for the energy prediction; however, it must be considered that this error can impact the charging/discharging plans and schedules of the EVs.

4. Characterization of Renewable Sources Generation Profiles

According to the optimization constraint of Eq. (6j) the other required input is the variable $\boldsymbol{P_{rn}^M} \in \mathbb{R}^n$ that indicates the predicted generation of renewable sources located at the charging stations at each time step.

In this case it was considered that the charging station contains 5 photovoltaic modules of 990 Wp with a peak power of 4.95 kWp and the estimation of the energy generated was performed with the model presented in [19] which has as inputs, the horizontal incident solar radiation and the temperature. The time series of both variables were taken from the database of reference [20] for the city of Texas since the data for Colombia were not available for the required time resolution of 5 minute intervals.

Subsequently, upon obtaining the photovoltaic energy generation time series, implementation of a Long Short-Term Memory Network (LSTM) ensued to predict the future behavior of renewable energy generation. The illustrated structure for the LSTM can be found in Fig. 4, featuring 4 sequential dropout layers comprising 48 neurons and 1 dense layer.
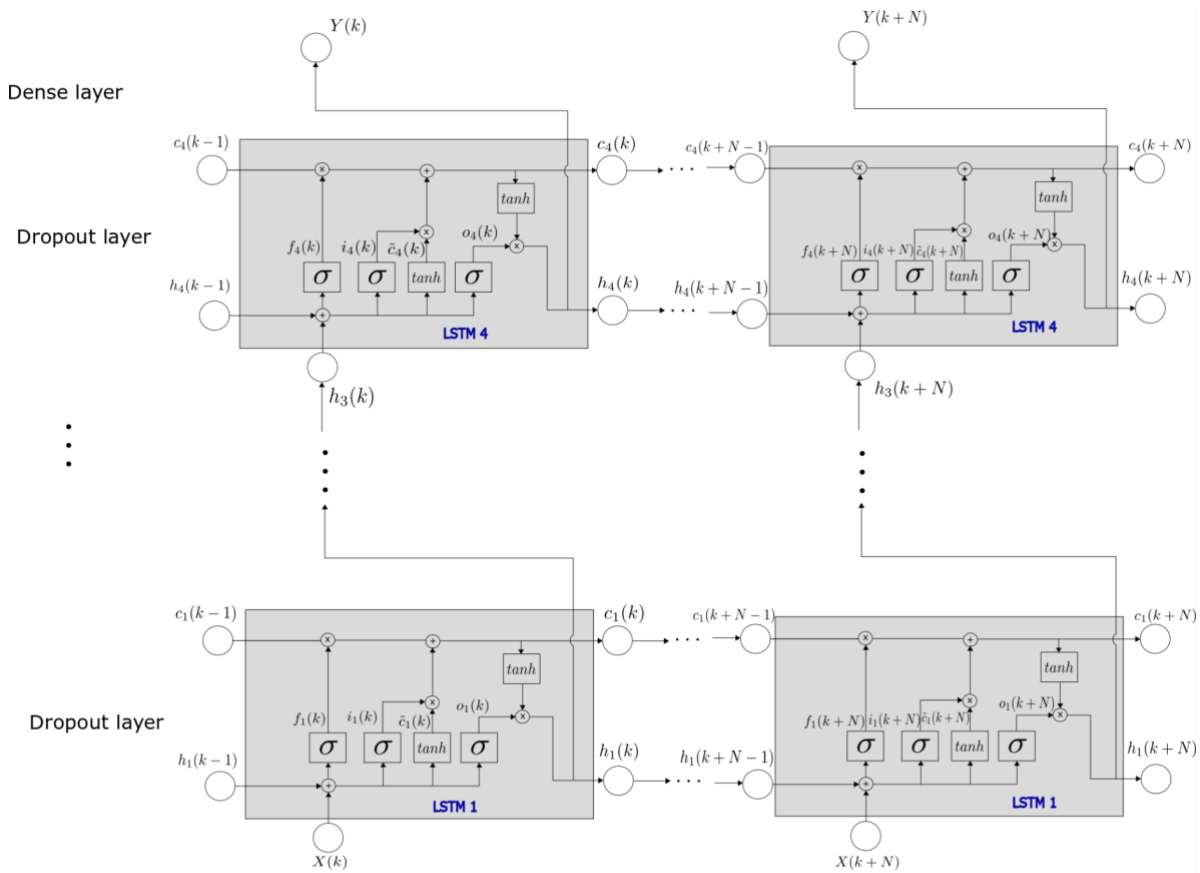
$$X(k) \in R^8, \quad N_s = 4032, \quad Y(k) \in R^1$$
$$h_j(k), \quad c_j(k), \quad f_j(k), \quad i_j(k), \quad \tilde{c}_j(k), \quad o_j(k) \in R^h$$
$$h = 48, \quad j \in \{1,...,4\}$$

Figure 4. LSTM network architecture for the prediction of renewable generation.

Being $\boldsymbol{X}$ the input dataset that has a dimension of 8×4032, where the first dimension corresponds to the number of segments of the time series stacked in time and delayed by 1 time step, and the second dimension corresponds to the length of these blocks, i.e. the training window that corresponds to a period of two weeks; $\boldsymbol{Y}$ the output dataset with size 1×4032. $h = 48$ the number of neurons of the individual LSTM units, $j = 4$ the number of sequential layers, $\boldsymbol{h_j} \in \mathbb{R}^h$ the hidden state vector, $\boldsymbol{c_j} \in \mathbb{R}^h$ the cell state vector, $\boldsymbol{f_j} \in \mathbb{R}^h$ the forget gate's activation vector, $\boldsymbol{i_j} \in \mathbb{R}^h$ the forget input/update gate's activation vector, $\hat{\boldsymbol{c}}_j \in \mathbb{R}^h$ the cell input activation vector, and $\boldsymbol{o_j} \in \mathbb{R}^h$ output gate's activation vector.

It is essential to note the distinction in architecture between the BPN and LSTM networks. The BPN has a simpler structure compared to the LSTM network. Unlike the conventional BPN, which treats the time dimension as a feature, the LSTM employs various processing elements or blocks designed to efficiently learn long-term dependencies.

Additionally, the LSTM network incorporates feedback loops among its elements over time, illustrated in Fig. 4 for variables *h* and *c*. These characteristics make the LSTM more suitable for renewable generation forecasting since it present rapid changes in time. [21]. The obtained forecasting results with the LSTM network, for the considered data, are shown in Fig. 5, which has an MSE error of 1.89 %.
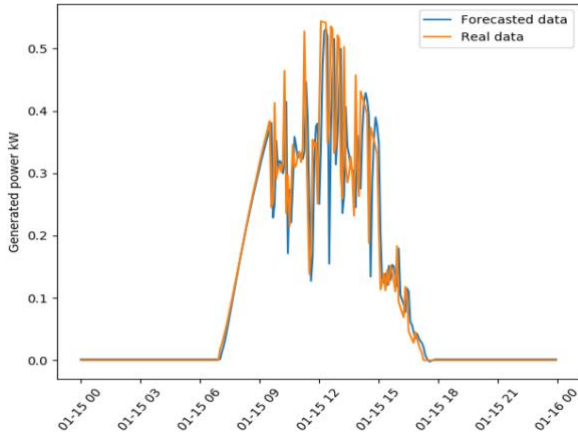
Figure 5. Predicted photovoltaic generation obtained with the LSTM network.

5. Study Case and Optimization Results

5.1. Study Case

The system chosen as a case study was composed of an existing public transport route in Medellín, Colombia, featuring proposed electric buses as its vehicles. The selected route, named "195II - Laureles Campestre - Estación Santa Lucía," was illustrated in Fig. 6. It has a length of 8 km and an average travel time of 20 minutes. The electric buses selected to supply the transport requirements of this route are a fleet of 3 rapid transit buses with 324 kWh, whose parameters are detailed in reference [22].
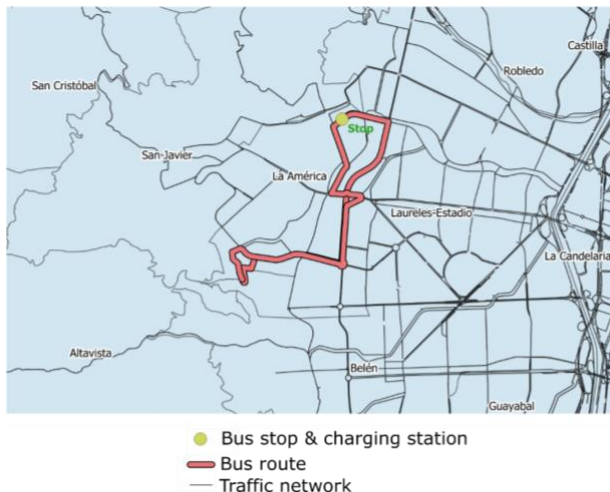
Figure 6. Illustration of the study case route and traffic network.

Furthermore, it is considered that the buses are dispatched with a frequency of 30 minutes between 5:00-21:00 h, and a frequency of 15 minutes the rest of the day.

Considering such elements, the energetic consumption of the EVs in the route, used to train the NN of Fig. 2, was obtained from performing traffic microsimulations of the study case zone and getting the speed, acceleration, and road slope profiles of each EV, for 63 different traffic congestion scenarios. The rest of the traffic interacting demand in each scenario (different from the EVs in the route) was estimated with the procedure described in [7].

Moreover, the parameters required in the objective function of the optimization in Eq. (6), such as the electricity cost, the revenues from energy sales, and the revenues from ancillary services provision were taken from reference [7]. And, the data for the estimation of the renewable generation, illustrated in Fig. 5, was taken from the reference [20] considering there were 5 photovoltaic modules in the charging station that can charge the vehicles parked at a specific time step.

5.2. Results and Analysis

This section presents the obtained decision variables derived from the solution of the Mixed-Integer convex optimization described in Eq. (6) for a daily time horizon with discrete intervals of 5 minutes. This procedure was carried out in the Matlab software using the Gurobi solver [23].

Fig. 7 shows the resulting energy in the EVs batteries for the high congestion scenario.
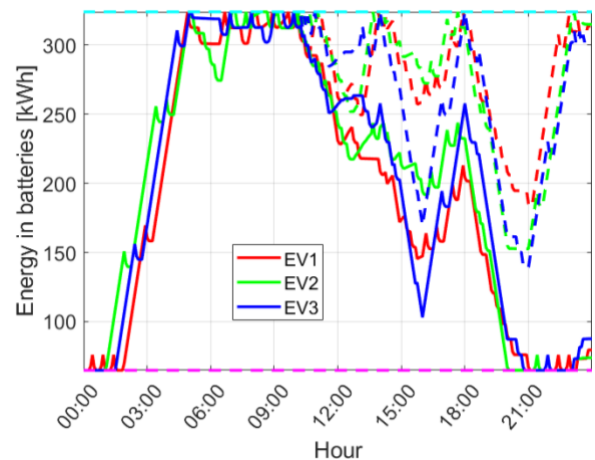
-Energy without provision of ancillary services.

-- Energy with provision of ancillary services.

Figure 7. Energy in EVs batteries for the different congestion scenarios.

From this figure, it is observed that the energy content of EVs is higher when the ancillary services provision is not considered (dashed line). This occurred because the upward and downward reserves deplete the batteries' capacities; however, even under the provision of such reserves, the energy content is higher than the minimum allowed, accomplishing the limit imposed by the constraints of Eq. (6b). However, it is important to highlight that the fulfillment of the energy constraints depends on the accuracy of the

energy expenditure and renewable generation estimations. In this case, accuracies of 0.12% and 1.89% were obtained for respective predictions using BPN and LSTM networks. However, deviations between real values and their predictions could potentially lead to vehicles running out of power, particularly at critical times such as between 9:00 p.m. and 2:00 a.m.

On the other hand, in Fig. 7, it was noted that the difference between the energy content with and without ancillary services provision increased after 10:00h. This happened because the optimization system considers an hourly varying electricity price that has higher values between 10:00 -22:00 h, as depicted in Fig. 8a which also illustrates the hourly energy purchased from the electrical network, sold, and stored for the provision of upward and downward reserves. It was observed that vehicles purchased energy during hours with lower electricity prices and sold energy during peak hours, ensuring that the exchanged power remained below the maximum allowed.
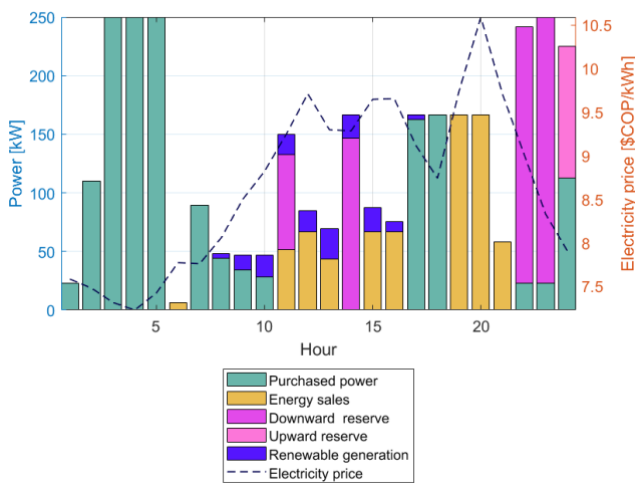
Furthermore, it was noticed that the downward reserve was scheduled during hours with lower electricity prices, as the EVs aimed to reduce the charging power while maximizing the reserve usage. Specifically, it was economically profitable for the EVs to schedule a charging surplus capacity in the next hours 8:00 h, 11:00 h, 14:00 h, 17:00 h in which the energy was cheap and also the reserves had a high probability of being used, according to [7] . A similar situation occurs in the upward reserve scheduling, as the EVs provided upward reserves at 23:00 h which was the time where is the upward reserves usage was more likely according to [7].

Additionally, Fig. 8b illustrates the total energy purchased, energy sold, and ancillary services provided for the two congestion scenarios depicted in Fig. 3. A conclusion derived from it is that as high is the network congestion more energy should be purchased, less energy can be sold, and lower downward reserves can be provided.

(a)
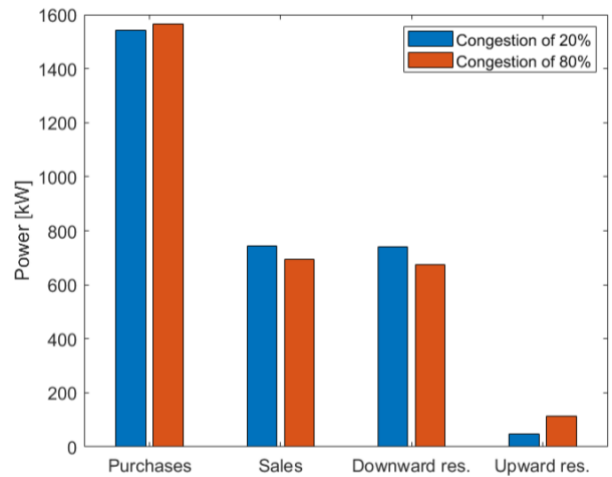
(b)

Figure 8a. Power generated and exchanged with the electrical network. Fig. 8b. Comparison of energy purchased, sold, and provided for ancillary services for the different congestion scenarios.

This is a consequence of the fact that in general, trips use more energy when there is more congestion on the network. However, in this case, the upward reserves could be increased because, in the case of greater congestion, the vehicles recover more energy from regenerative braking at 2:00 p.m. (see fig. 3), so they can use this surplus energy as an ancillary service. Moreover, it is remarked that, despite the fact that in the data accumulated for the entire fleet of EVs given in Fig. 8, the charging and discharge of the batteries occur simultaneously (for example at 3:00 p.m. where the vehicles are charged with renewable energy and they also sell energy to the grid), this does not happen at the level of each vehicle, because thanks to the constraints given in Eqs. (6.e) - (6.f) the same vehicle cannot be charged and discharged at the same time, as well as it cannot interact with the power network when it is dispatched

for travel. But in Fig. 8 this phenomenon is noted because while some vehicles are loaded, others are unloaded or dispatched for trips, it can be seen for example at 5:00 a.m. in Fig. 7.

Additionally, it is noted that a sensitivity of the solution regarding the congestion level variations is appreciable in Fig. 9; specifically, the optimal value changes a 3.64% when the congestion is decreased from 80% to 20%; and changes a 1,4% when the photovoltaic generation is calculated with the real measured data presented in Fig. 5. These facts confirm that the estimation errors in the energy expenditure and the photovoltaic generation impact, not only the constraints accomplishment but also the solution of the optimization.

Finally, the average running time of the dynamic optimization, for the cases evaluated was 1,302.5 seconds or 21.7 minutes, exceeding the length of the time steps (5 minutes). This indicates that the proposed algorithm is suitable for offline execution. However, simulation time can be reduced by increasing the length of time steps, enabling its application for online management purposes.

6. Conclusions

This paper presents a management strategy for a fleet of public transport EVs that sell energy and provide frequency regulation ancillary services to the electrical network. The strategy integrates two artificial intelligence prediction algorithms with a decision-making system based on Mixed-Integer dynamic optimization, which takes the predictions as inputs.

The first artificial intelligence prediction algorithm based on a BP neural network was trained to forecast the energy expenditure of EVs in travels according to their departing schedule and the average traffic congestion in the analysis region for the specific calculation day, which are inputs available or whose obtaining is suitable for public transport systems. The second prediction algorithm, based on an LSTM network, was trained to forecast solar energy production from photovoltaic modules installed at the charging station, using radiation samples from two weeks ago as input. Moreover, the findings from the optimization result demonstrated a dependency between the feasibility of the solution, the reached optimum value, and the estimator's accuracy. Therefore, it emphasizes the importance of employing high-accuracy algorithms, as presented in this paper, during the prediction stage to mitigate the risk of operational failures.

One of the key advantages of the proposed strategy is its capability to provide individual charging/discharging and dispatch plans for each EV, even suggesting which vehicle must perform a required route, considering that vehicles must operate in the point that allows the whole fleet to be at the most profitable operative condition. This suggested operative condition considers not only economic factors of energy purchase, sale, and provision of ancillary services, but also takes into account the cost of batteries' wear, which avoids abrupt changes in the state of charge of the EVs. On the other hand, the developed strategy was proposed for an offline day ahead EVs management for a system with a single charging station, but the same model can be brought to online applications increasing the time step of the calculation, keeping in mind that it also could reduce the accuracy of the optimization model.

Besides, the proposed model can be adapted, in future works, to multi-charging stations systems, adding dynamic equations for representing the vehicle's flow among stations and the energy expenditure for the different travel directions.

Acknowledgments

References

[1] J. Kang, S. J. Duncan, and D. N. Mavris, "Real-time scheduling techniques for electric vehicle charging in support of frequency regulation," *Procedia Comput. Sci.*, vol. 16, pp. 767–775, 2013.

[2] G. Caneponi, F. Cazzato, S. Cochi, M. Di Clerico, M. C. Falvo and M. Manganelli "EV Charging Stations and RES-Based DG : a Centralized Approach for Smart Integration in Active Distribution Grids," *Int. J. Renew. Energy Res.*, vol. 9, no. 2, 2019.

[3] S. Ruiz-Álvarez and J. Espinosa, "Multi-Objective Optimal Sizing Design of a Diesel- PV-Wind-Battery Hybrid Power System in," *Int. J. Smart grid*, vol. 2, no. 1, 2018.

[4] N. Rotering and M. Ilic, "Optimal charge control of plug-in hybrid electric vehicles in deregulated electricity markets," *IEEE Trans. Power Syst.*, vol. 26, no. 3, pp. 1021–1029, 2011.

[5] T. Harighi, R. Bayindir, and E. Hossain, "Overviewing Quality of Electric Vehicle Charging Station's Service Evaluation," *Int. J. Smart grid*, vol. 2, no. 1, 2018.

[6] Santoshkumar and R. . Udaykumar, "Development of Wireless Access Support for EV to Smart Meter Communication in Vehicle-to-Grid," *Int. J. Renew. Energy Res.*, vol. 5, no. 2, 2015.

[7] S. Ruiz-Alvarez, "Methodology to design an optimal decision making system for the operator of a shared electric vehicle fleet providing electrical ancillary services," Universidad Nacional de Colombia, 2021.

[8] M. G. Vayá, L. B. Roselló, and G. Andersson, "Optimal bidding of plug-in electric vehicles in a market-based control setup," in *Proceedings - 2014 Power Systems Computation Conference, PSCC 2014*, 2014.

[9] E. Sortomme and M. A. El-sharkawi, "Optimal Scheduling of Vehicle-to-Grid Energy and Ancillary Services," *IEEE Trans. Smart Grid*, vol. 3, no. 1, pp. 351–359, 2012.

[10] R. J. Bessa and M. A. Matos, "Global against divided optimization for the participation of an EV aggregator in the day-ahead electricity market. Part II: Numerical analysis," *Electr. Power Syst. Res.*, vol. 95, pp. 309–318, 2013.

[11] A. T. Al-Awami and E. Sortomme, "Coordinating vehicle-to-grid services with energy trading," *IEEE Trans. Smart Grid*, vol. 3, no. 1, pp. 453–462, 2012.

[12] H. Turker, A. Radu, S. Bacha, D. Frey, J. Richer, and P. Lebrusq, "Optimal charge control of electric vehicles in parking stations for cost minimization in V2G concept," *3rd Int. Conf. Renew. Energy Res. Appl. ICRERA 2014*, pp. 945–951, 2014.

[13] H. Turker, I. Colak, and B. T. Gelistirme, "Multiobjective optimization of Grid – Photovoltaic

– Electric Vehicle Hybrid system in Smart Building with Vehicle-to-Grid (V2G) concept," *2018 7th Int. Conf. Renew. Energy Res. Appl.*, vol. 5, pp. 1477–1482, 2018.

[14]   A. Damiano, C. Musio, and I. Elettrica, "A Microgrid Energy Management System Supported by a Hysteresis Vehicle to Grid Controller," *4th Int. Conf. Renew. Energy Res. Appl.*, vol. 5, pp. 879–884, 2015.

[15]   A. Amirkhani, A. Haghanifar, and M. R. Mosavi, "Electric Vehicles Driving Range and Energy Consumption Investigation: A Comparative Study of Machine Learning Techniques," *5th Iran. Conf. Signal Process. Intell. Syst. ICSPIS 2019*, no. December, pp. 18–19, 2019.

[16]   D. Aguiar, M. Palacio, D. Hernández, and J. Manosalva, "Medellin y su calidad del aire," *Esc. Int. Desarro. Sosten.*, 2016.

[17]   D. Kumar, H. D. Mathur, S. Bhanot, and R. C. Bansal, "Forecasting of solar and wind power using LSTM RNN for load frequency control in isolated microgrid," *Int. J. Model. Simul.*, vol. 41, no. 4, pp. 311–323, 2021.

[18]   D. Swain, Vijeta, S. Manjare, S. Kulawade, and T. Sharma, "Stock Market Prediction Using Long Short-Term Memory Model," *Adv. Intell. Syst. Comput.*, vol. 1311 AISC, pp. 83–90, 2021.

[19]   N. M. Bellaaj, "Optimal Sizing Design Of An Isolated Microgrid Using Loss Of Power Supply Probability," *2015 6th Int. Renew. Energy Congr.*, 2015.

[20]   National Renewable Energy Laboratory, "NSRDB: National Solar Radiation Database," *NSRDB: National Solar Radiation Database*, 2021. [Online]. Available: https://nsrdb.nrel.gov/. [Accessed: 05-Jan-2022].

[21]   G. Van Houdt, C. Mosquera, and G. Nápoles, "A review on the long short-term memory model," *Artif. Intell. Rev.*, vol. 53, no. 8, pp. 5929–5955, 2020.

[22]   S. Ruiz, N. Arroyo, A. Acosta, C. Portilla, and J. Espinosa, "An Optimal Battery Charging And Schedule Control Strategy For Electric Bus Rapid Transit," in *Proceedings of Joint Conference MOVICI - MOYCOT 2018*, 2018.

[23]   Gurobi Optimization, "Gurobi optimizer," *Gurobi Optimization*, 2016. [Online]. Available: http://www.gurobi.com/documentation/6.5/refman.pdf.